A&A 375, 661–669 (2001)
DOI: 10.1051/0004-6361:20010707

Astronomy & Astrophysics

Stability of the extragalactic VLBI reference frame*

A.-M. Gontier[1], K. Le Bail[1,2], M. Feissel[1,2], and T. M. Eubanks[3,**]

[1] Observatoire de Paris/CNRS UMR8630, 61 Av. de l'Observatoire, 75014, Paris, France
[2] Institut Géographique National/LAREG, 8 Av. Blaise Pascal, Champs sur Marne, 77455 Marne la Vallée Cedex 2, France
[3] US Naval Observatory, code EO, Massachusetts Avenue, NW, Washington, DC 20392-5420, USA

Received 22 September 2000 / Accepted 1 March 2001

Abstract. The qualification and the maintenance of the International Celestial Reference Frame (ICRF) source directions are currently based on global statistics regarding the complete data set of VLBI observations of extragalactic radio sources. The founding hypothesis in the selection of extragalactic objects to access a quasi-inertial reference system is that their directions are fixed in space. Therefore the study of the time variability of the sources is an important step in the process of checking and improving the reliability of the ICRF, in view of high precision applications such as Earth rotation studies or the unification with future space astrometry results. In this paper we investigate the systematic and random behaviours in time series of individual determinations of coordinates for several hundred sources over 1987–1999. New criteria for the qualification of sources in a future revision of the ICRF are proposed.

Key words. quasars – techniques: interferometric – astrometry – reference systems

1. Introduction

The IAU recommended in 1997 the use of the International Celestial Reference System (ICRS) as the conventional celestial reference system (see Feissel & Mignard 1998), determined using the coordinates of compact extragalactic radiosources observed with VLBI, the International Celestial Reference Frame (ICRF). The initial realization of the ICRS was published in 1997 (Ma et al. 1998; see also Ma & Feissel 1997). It includes 608 objects, two thirds of which are quasars and the rest mainly BL Lac objects and galaxies. The most recent update and extension, ICRF-Ext.1, is now available with 667 objects (IERS 1999). The computation for ICRF-Ext.1 is based on the same analysis options as those for ICRF (Ma 2000).

The radiosource coordinates in ICRF and ICRF-Ext.1 are derived from the complete set of observations over 1979–1999. They are qualified in two ways, 1. by ascribing realistic uncertainties that take into account both the random and systematic errors – a floor of 0.25 mas in $\alpha \cos\delta$ and δ was ascribed to the published position uncertainties to account for residual modelling errors – and 2. by categorizing them, in decreasing order of confidence, as "defining", "candidates", and "other". This complex assessment scheme is made necessary by the existence of variations in the apparent directions of the sources.

The above lower limit is considered valid for source positions obtained over many years of observations. Thanks to the availability of the session-per-session coordinates of over 600 sources of ICRF-Ext.1, it is possible to investigate the source stability in a time series approach. A detailed case study of 16 sources north of $+20°$ selected from this data file (Feissel et al. 2000) seems to indicate that in the best conditions the effective coordinate accuracy could reach values smaller than 0.1 mas for yearly averages.

In this paper, we investigate the systematic and random characteristics of several hundred source apparent motions in order to derive a set of qualifiers that would be helpful in selecting sources to maintain a precise and stable celestial reference frame. We show an example of a statistical source selection algorithm that stabilizes the reference frame. We then compare the outputs of the various selection criteria, the current ICRF ones and several others based on this study.

2. Time series of source coordinates

For historical reasons, the number of observations per source are extremely uneven. Some bright sources that were used to provide reference directions in the early

Send offprint requests to: A.-M. Gontier,
e-mail: Anne-Marie.Gontier@obspm.fr

* Table 2 is only available in electronic form at the CDS via anonymous ftp to
cdsarc.u-strasbg.fr (130.79.128.5) or via
http://cdsweb.u-strasbg.fr/cgi-bin/qcat?J/A+A/375/661

** now at Multicast Technologies.

years of VLBI appeared too variable or too extended after some years and were discarded, to the benefit of other, fainter sources that became usable thanks to progress in technology. Some sources considered as best fitting the astro-geodetic needs are repeatedly observed, while others, considered less useful for this purpose, are observed less frequently, mainly for astrometry studies.

Our study is based on the computed coordinates of the radiosources in a homogeneous reference frame, with one determination for each of the sessions in which the source was observed. This computation was done at the US Naval Observatory (Washington) using the CALC-SOLVE software. Figure 1 shows the histograms of rates of observation for the 208 most regularly observed sources over 1988–1999. These sources provide the backbone of the ICRF. About half of them have fewer than 1500 observations in less than 60 sessions. Twenty-one sources have more than 30 thousand observations in more than 1000 sessions.

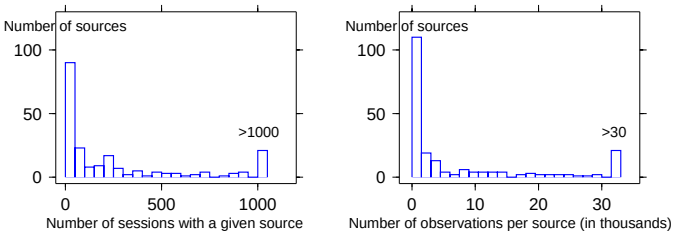

Fig. 1. Histograms of rates of observations over 1988–1999 for the 208 best observed ICRF sources.

2.1. Systematic variability and deformations

According to Ma et al. (1998) there are two major causes of the current limitation in accuracy of VLBI source positions.

- Tropospheric delay modelling. The uncertainty in the modelling of the propagation delay due to the wet component of the troposphere, combined with deficiencies in the network geometry (majority of stations in the northern mid-latitudes, short N-S components of the baselines yielding the observation of low declination objects at low elevation, where the mis-modelling of the delay has the largest effect), may give rise to baseline-dependent systematic errors in declinations. This is illustrated in Fig. 2, which shows the influence on declinations of correcting the observations for the effect of the greater troposphere thickness nearer the equator ("gradient function correction", see McMillan & Ma 1997). The quasi-symmetry of the declination effect with respect to the equator reflects the structure of both the atmosphere and the observing network.
- Source structure. No radiosource is really point-like when observed in centimetric wavelength with baseline lengths around 6000 km. If the source structure is extended or is not circular, its apparent direction may change as a function of the length and orientation of the baselines. In addition, the source structure usually changes with time. In principle it is possible to accurately correct this effect, provided that repeated maps of the sources are available (Charlot & Sovers 1997). In the framework of the ICRF maintenance, a systematic program for source mapping and astrometric correction computation is under way (Fey & Charlot 1997, 2000). However, the correction procedure is not routinely used in the existing global analysis software. This mismodelling is expected to propagate errors into the source positions up to the level of 0.2 mas.

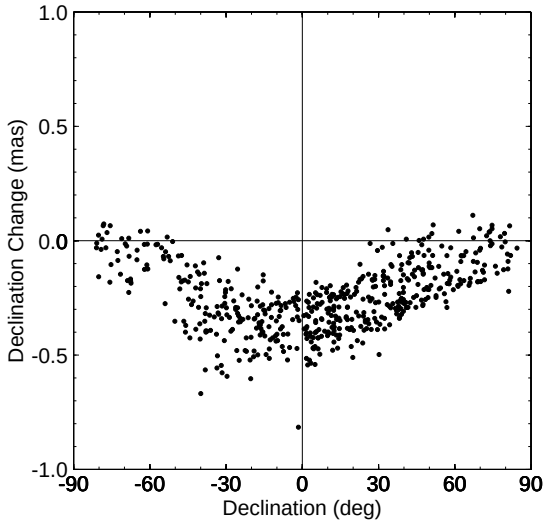

Fig. 2. Effect of tropospheric gradients on declinations as a function of declination, reproduced from Ma et al. (1998).

The above two effects are expected to contribute coloured noise to the error spectrum of the observed data.

In order to use standard time series statistics to investigate the systematic and random variability of source directions, the original series of coordinates with irregular spacing are first transformed into equally spaced series by performing weighted averages. Averaging times of 0.5 year and 1 year are used in this paper.

The VLBI results are expressed in the equatorial system of coordinates (right ascensions and declinations), which is linked to the Earth's rotation axis and has no particular relationship with the source geometry. On the other hand, most of the known activity of quasars takes the form of jets, i.e., aligned emissive structures that cause an apparent motion of the observed emission centre relative to a fixed background. In parallel, noise in declination will also simulate an aligned structure, that may or may not hide the real source structure effect. In order to take into account this specific character of the expected apparent variabilities, we define a local system of axes in which the source instability will be studied. These axes have their origin at the mean source coordinates, the x-axis being in the direction of maximum standard deviation of the set of 0.5 year weighted averaged coordinates over 1987.25–1999.25, and the y-axis forming a direct rectangular system with it. Then we define a "variability envelope"

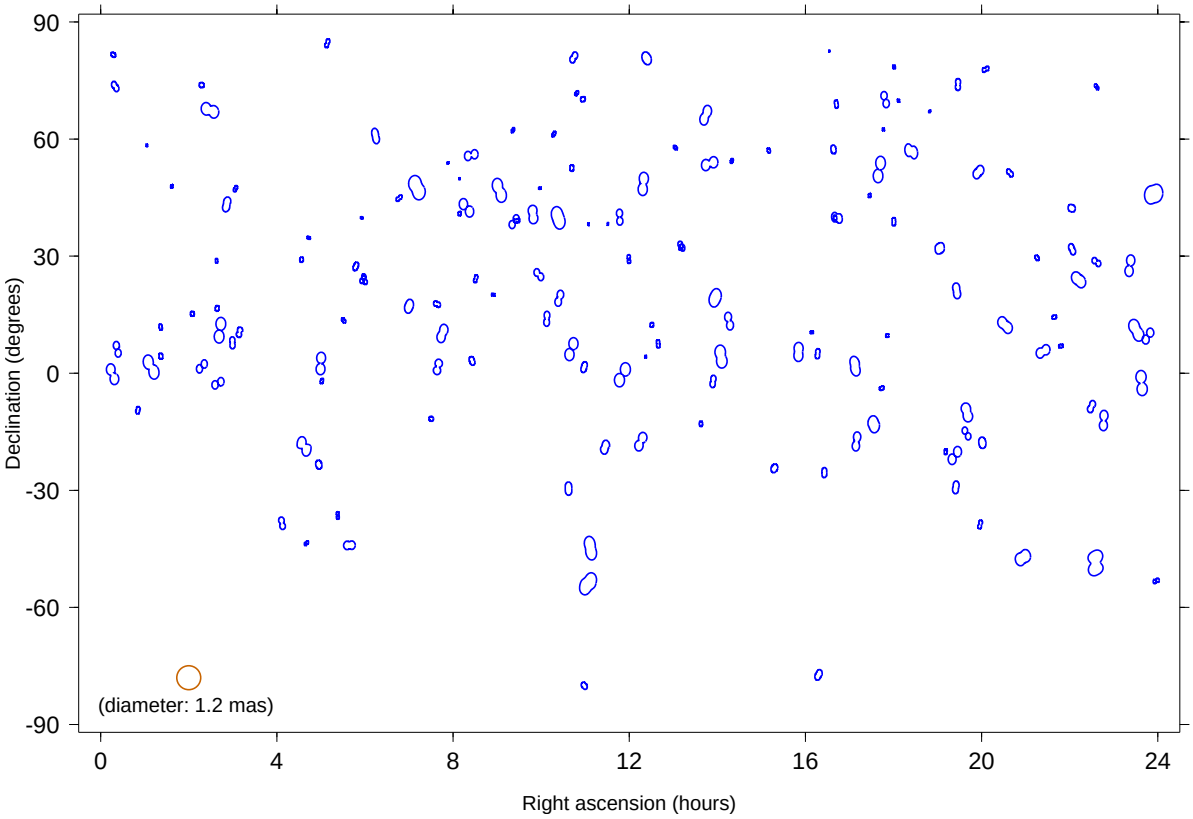

Fig. 3. Sources with high or moderate stability. The figure shows the envelopes of the 1987–1999 standard deviation of 0.5 year averages in equatorial coordinates. Abscissae: $\alpha \cos\delta$, ordinates: δ. The scale is given by the circle (lower left).

as the contour generated in the local frame by vectors centered at the origin and whose length is the standard deviation of the time series of coordinates projected in all directions of the plane.

About 250 sources are found to have a dense enough observational history over 1987–1999 to derive the envelope of their local variability. Figure 3 (resp. 4) shows the local variability envelopes corresponding to 0.5-year averaging intervals, in the equatorial reference frame, for sources with a standard deviation at 0.5-year intervals smaller (resp. larger) than 0.6 mas. Most envelopes are elongated, as would be expected from the active jet structure of the sources.

Superimposed on this shape, one can notice a closer alignment of the local x-axis with the declination direction, particularly visible for the less stable sources (Fig. 4). Table 1 gives the distribution of *the angle of the x-axis* (axis of maximum local variability) *with the declination axis*, for sources shown in Figs. 3 and 4. The set of the most stable sources shows a quite even distribution of the local directions of maximum variability in the declination zones north of +20°and south of −20°, suggesting that the observed variability corresponds to real local effects in the sources. However, the results in the declination zone [−20°, +20°] show an excess of variability in the direction of declinations, probably reflecting the tropospheric mismodelling mentioned above. This excess is much stronger for the more variable sources, for which an even distribution is reached only north of +20°.

Table 1. Distribution of the angles of the axes of maximum local variability with the declination axis, for sources shown in Figs. 3 (stable sources) and 4 (unstable sources).

Declinations	Inclination bins (absolute values)					
(degrees)	0°–30°		30°–60°		60°–90°	
	Stable	Unst.	Stable	Unst.	Stable	Unst.
]+20°, +90°]	35%	32%	42%	45%	23%	23%
]0°, +20°]	55%	55%	27%	31%	18%	14%
]−20°, 0°]	55%	67%	30%	20%	15%	13%
[−90°, −20°]	42%	70%	26%	18%	32%	12%

These noise features reflect the medium frequency (0.5-year intervals) effect of the known systematic declination errors due to the troposphere modelling. The global impact of these deformations on a reference frame materialized by the source coordinates can be modelled as a constant offset in the declinations (see Sect. 3).

Another view to qualify the systematic part of the source instability is the estimation of *linear rates* in the coordinates. To the extent that they are related to the source structure, such drifts are expected to take place in the direction of the maximum variability (the above defined local x-axis). The drifts along the local x-axis are listed in Table 2 (column "rate") and shown in Fig. 5. The idea of looking for a drift in the source coordinates is somewhat

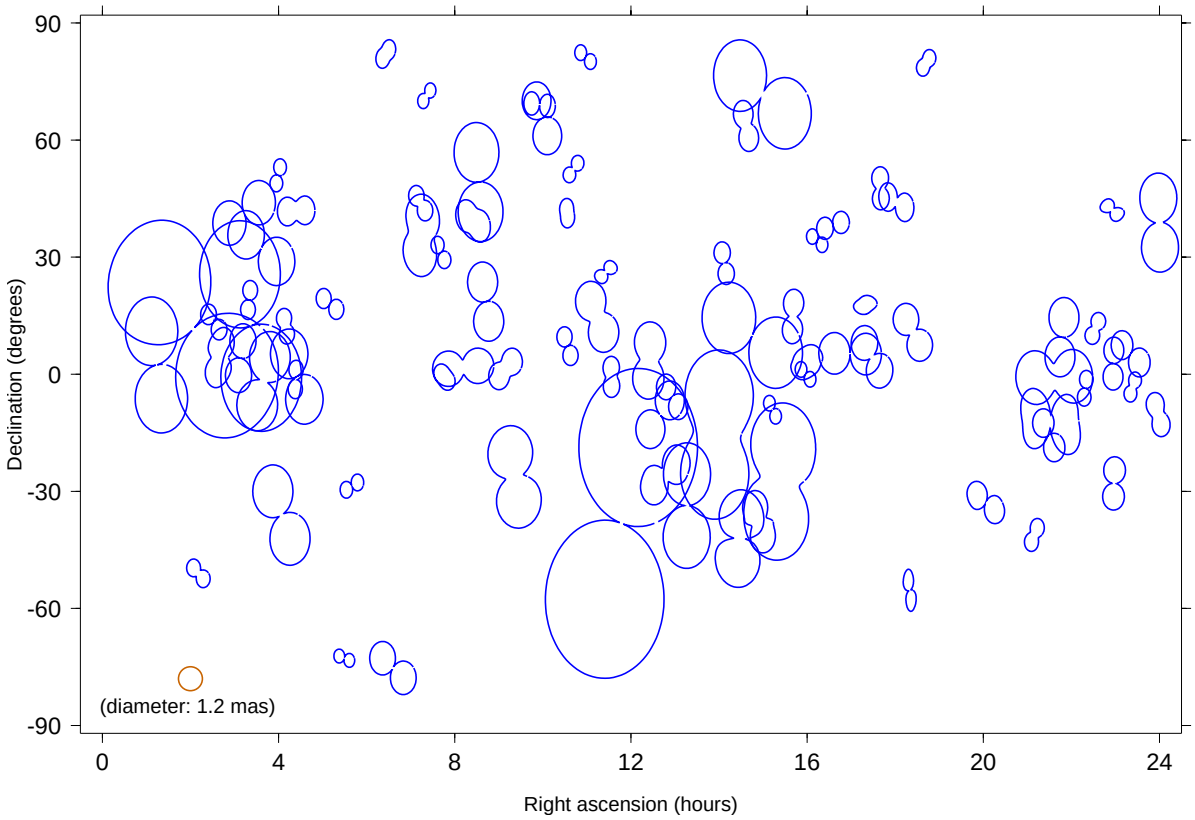

Fig. 4. Sources with low stability. The figure shows the envelopes of the 1987–1999 standard deviation of 0.5 year averages in equatorial coordinates. Abscissae: $\alpha \cos\delta$, ordinates: δ. The scale is given by the circle (lower left).

difficult to justify in the long run, if one considers the expected causes for it. Phenomena generally invoked are 1. the changing emission structure, and 2. gravitational lensing by matter crossing the line of sight. A drift caused by source structure changes is in principle limited by the size of the brightest portion of the structure. It will appear as linear or quasi linear only if the observation span (12 years in our case) is short with respect to the characteristic time of the phenomena involved.

2.2. Random variability

The random variability of the source coordinates can be characterized by the χ^2 *test*. The statistics are given in Table 2 (column "χ^2"). A rigorous χ^2 test (Bevington 1969, p. 187) can be performed on the individual session-weighted coordinates only for sources recorded in at least 100 sessions, about 100 sources. The histograms of the estimated χ^2 are shown in Fig. 6. These highly observed sources obtain reasonable values of χ^2, 77% of them have a χ^2 smaller than 2.5 in $\alpha \cos\delta$ and 62% in δ.

To enlarge the set of sources scrutinized by a χ^2 test, we also consider the yearly average coordinates. In this case, because of the small number of years, the estimator is the so-called "*goodness of fit (gof)*", defined by the following relationship (Bevington 1969, p. 188):

$$gof = \frac{1}{N-1} \sum_i \frac{r_i^2}{\sigma_i^2} \qquad (1)$$

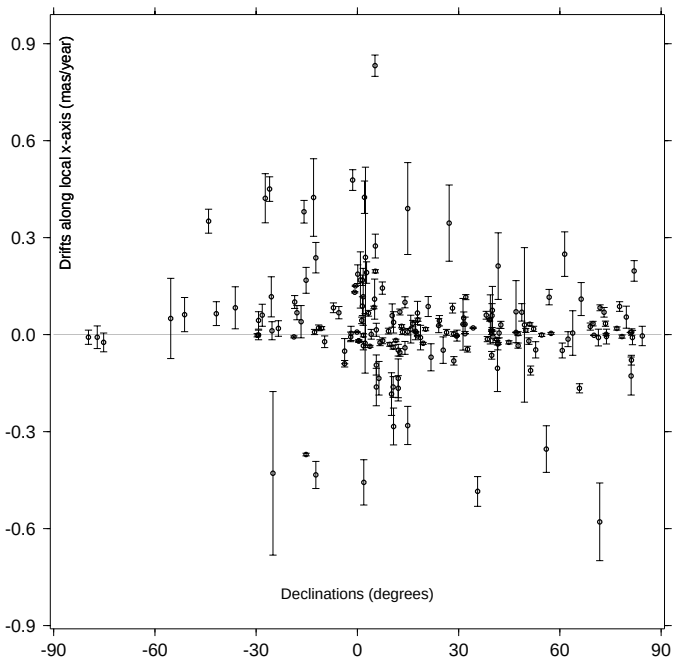

Fig. 5. Linear drifts of 187 source positions over 1987–1999 (in mas/year) in the direction of maximum variability.

where r_i are the yearly average coordinates for years i, σ_i are their standard deviations, and N is the number of years where the source has observed coordinates. A goodness of fit near to 1 indicates white noise. In the context of time series, white noise corresponds to

frequency-independent variance. Large values of the goodness of fit mark an increased noise at lower frequencies. The values of this estimator are listed in Table 2 (column "*gof*") and their histograms are shown in Fig. 7. As can be expected, the largest values of the goodness of fit are associated with the axis of maximum local variability. In the perpendicular direction however, about 70% of the sources have a goodness of fit smaller than 2.5. This last direction is the least sensitive to the two main sources of systematic errors. The goodness of fit in their direction might be considered as an indicator particularly sensitive to random errors.

The *spectral characteristics* of the time series of source coordinates are also investigated using the Allan variance method (Allan 1966; see a review of these methods in Rutman 1978). The Allan variance analysis allows one to characterize the power spectrum of the variabilities in time series, for sampling times ranging from the initial interval of the series to 1/4 to 1/3 of the data span, in our case 6-months to 3–4 years. This method allows us to identify white noise (spectral density S independent of frequency f), flicker noise (S proportional to f^{-1}), and random walk (S proportional to f^{-2}). Note that one can simulate flicker noise in a time series by introducing steps of random amplitudes at random dates. In the case of a white noise spectrum (an implicit hypothesis in the current ICRF computation strategy), accumulating observations with time eventually leads to the stabilisation of the mean position. In the case of flicker noise, extending the time span of observation does not improve the quality of the mean coordinates. Only 60 sources have observational histories that are dense enough to allow the investigation of the error spectrum using the Allan variance test. Table 2 (column "Sp") gives the result of the test in the direction of maximum local variability. About 60% of the series of coordinates have white noise and 40% have flicker noise. This classification is uncorrelated with the "definition/candidate/other" classification currently used in the ICRF maintenance process.

About 160 sources are observed sufficiently to derive a reliable Allan variance for a one-year sampling time, given in Table 2 (column "Av"). The Allan variance is the usual criterion used to qualify the stability of time series. The values found for this criterion are illustrated in Fig. 8. About 2/3 of the sources have a stability at one year intervals better than 250 μas in equatorial coordinates. This fraction increases to 9/10 in the direction perpendicular to that of maximum variability of the sources.

The results of the various tests and noise measurements performed in this study are gathered in Table 2. This table contains the 283 best observed sources, selected from the Eubanks (1999) data set on the basis of length and density of the time series of coordinates. The table is divided in three parts, with the left hand side giving general information and counts, the middle part giving statistics in the source local frame, and the right hand side giving statistics in the equatorial frame. The meaning of the column headings is as follows.

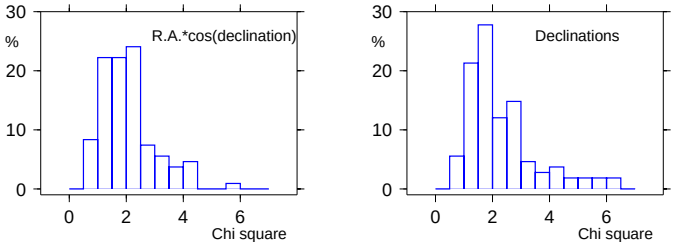

Fig. 6. Histogram of the χ^2 distance of series of source coordinates, in the equatorial coordinate system. Total: 108 sources.

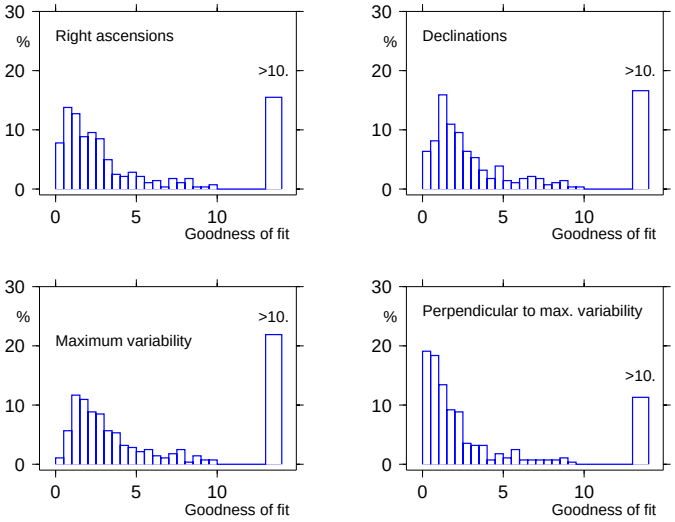

Fig. 7. Histogram of the goodness of fit of yearly averages in the equatorial coordinate system (top) and in the local one (bottom). Total: 283 sources.

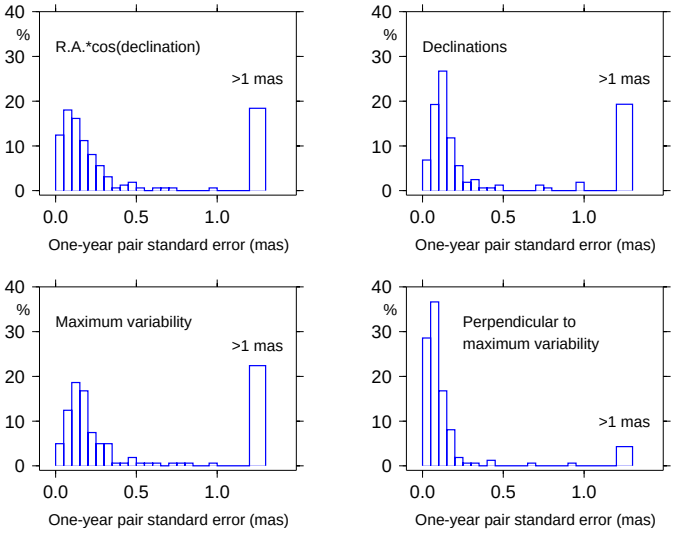

Fig. 8. Histogram of Allan standard errors of yearly averages in the equatorial coordinate system (top) and in the local one (bottom). Total: 161 sources.

- Source: IERS designation of the radio source.
- S: ICRF status of the source (**d**efinition, **c**andidate, **o**ther, **n**ew).
- Number of sessions with more than two observations of the source.

– Number of years with observations of the source in at least six sessions.

– ang: Angle of the axis of maximum local variability with the declination axis.
– *gof*: Goodness of fit of the yearly coordinate in the direction of maximum local variability.
– Av 1-yr: Allan standard error of yearly coordinate in the direction of maximum local variability.
– index (yr): Fey & Charlot source structure index and epoch of source structure index (years-1900).
– Sp: Spectral type of noise in the direction of maximum local variability: White noise (W) or Flicker noise (F).
– rate: Rate of apparent motion in the direction of maximum local variability (in mas/year).

Right ascensions

– χ^2: χ^2 of individual right ascensions (# marks poor estimates)
– *gof*: Goodness of fit of yearly right ascensions
– 1Av: Allan standard error of yearly $\alpha\cos(\delta)$

Declinations

– χ^2: χ^2 of individual declinations (# marks poor estimates)
– *gof*: Goodness of fit of yearly declinations
– 1Av: Allan standard error of yearly declinations.

3. Stabilizing the celestial reference frame

We adopt a time series approach in order to select sources that are stable enough to insure convergence of a global reference frame, based on several years of observations. Using the series of differences of yearly source coordinates with respect to the global mean coordinates for each source, we construct a series of yearly differential frames. We then compute the yearly differential rotation angles $A_1(y)$, $A_2(y)$, $A_3(y)$ around the axes of the equatorial coordinate system for year y, using the two following equations, where α, δ are the source coordinates and $\Delta\alpha(y)$, $\Delta\delta(y)$ are the differences of the average coordinates for year y with the mean source coordinates. The dz term is introduced to account for any residual equator bias resulting from the systematic errors in declination mentioned in Sect. 2.1.

$$\Delta\alpha(y) = A_1(y)\tan\delta\cos\alpha + A_2(y)\tan\delta\sin\alpha - A_3(y)$$
$$\Delta\delta(y) = -A_1(y)\sin\alpha + A_2(y)\cos\alpha + \mathrm{d}z(y).$$

The estimation of the four unknowns A_1, A_2, A_3 and dz is done at one-year intervals, both by weighted least squares (L2) and by minimizing residuals according to the L1 norm (absolute value of the residuals). The latter method is known to be less sensitive to outliers than the former. However, the global VLBI analysis computations from which celestial reference frames are derived are based on the L2 norm estimation. Therefore, in this context, the L1 norm estimation is only used for test purposes. In the estimations, the observation equations are weighted according to the variances of the yearly average coordinates.

Among the 283 sources documented in Table 2, 13 were discarded for the estimation of the rotation angle because of unreasonably large standard errors in the yearly coordinates. Starting with the 270 remaining sources, we implement a source selection algorithm based on the stability of the individual source coordinates as measured by the goodness of fit in the local x-axis direction (Table 2, column "*gof*" in the left-hand side section). For the set of sources under consideration, the time series of unknowns are estimated in both the L1 and L2 norms. The convergence criterion is based on the distance between the two solutions. Sources with the largest goodness of fit are progressively eliminated until the distances at all dates are smaller than the standard error of the L2 estimate (see Fig. 9).

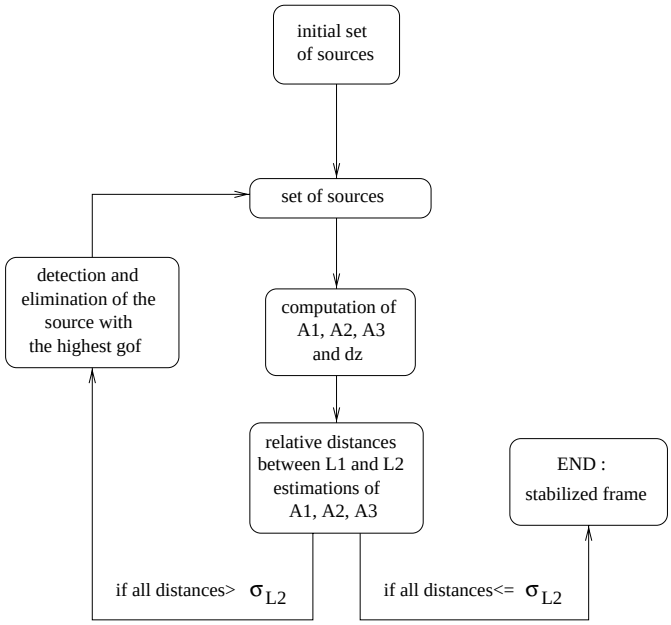

Fig. 9. Stability algorithm for a series of yearly differential celestial frames.

The algorithm stabilizes when 242 sources out of the original 283 are kept (86%), corresponding to a maximum goodness of fit of 17.5. The rms distance between the L1 and L2 estimates of A_1, A_2, A_3, that was at the level of 176 μas over the twelve years at the start of the process, then reaches 82 μas (114 μas over 1987–1992, 21 μas over 1993–1998).

Figure 10 shows the time series of the L2 estimates of the angles at the start and end of the stabilizing process. The effective numbers of sources present in each yearly solution are given with the A_2 graph (bottom line for the final selection, upper line for the initial set).

The better stability of the yearly reference frames in the second half of the time span is associated with the larger number of sources. Table 3 gives the stability of the A_1, A_2 and A_3 axes for the two half-intervals.

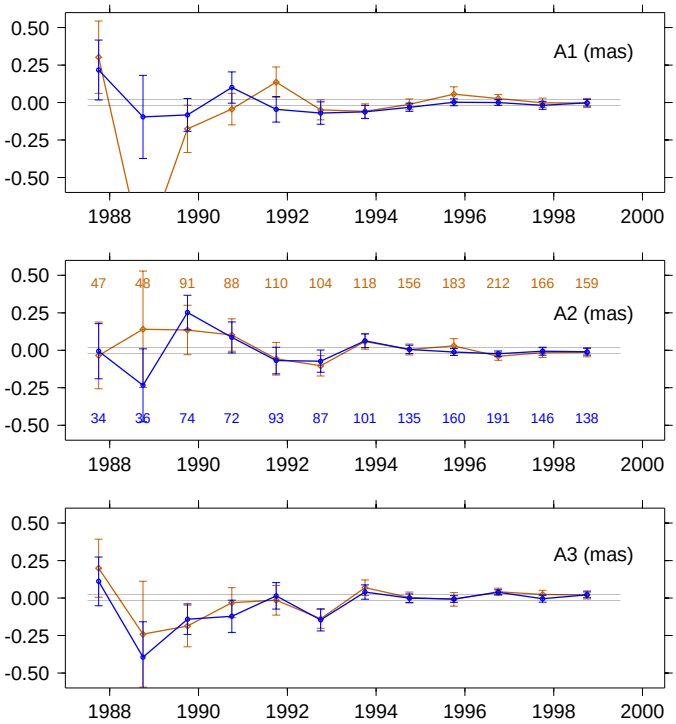

Fig. 10. Relative rotation angles of yearly CRFs, before (yellow/light) and after (blue/heavy) the implementation of the stabilizing algorithm. The double horizontal line corresponds to the stated uncertainty of the ICRF axes directions (± 20 μas).

The stability is at the level of ± 20 μas for the first six years, then drops to ± 3–4 μas over 1993–1998. These estimates of the celestial frame stability can be compared to the stated uncertainty of the ICRF axes (± 20 μas, shown in Fig. 10 by a double horizontal line), that was based on the comparison of reference frames obtained from subsets of the observations, with no consideration of time.

Table 3. Stability of the stabilized celestial reference frame in six-year intervals: A_1, A_2 and A_3 axes, and dz.

Time span	No of sources		A_1	A_2	A_3	dz
	Min	Max	(μas)	(μas)	(μas)	(μas)
1987–1992	34	93	14.4	20.7	22.9	16.6
1993–1998	101	191	3.4	3.3	4.1	2.8

Figure 11 shows the time series of the additional parameter dz at the start and end of the stabilizing process. While the deformation it reflects is quite sizeable in the early years, the effect practically disappears after 1992 (see also Table 3). The influence of the rejected sources is visible only before 1992. This suggests that, for the sources selected on the basis of continuity of observation, the instability before 1992 is due globally to the actual implementation of the technique rather than to the sources themselves.

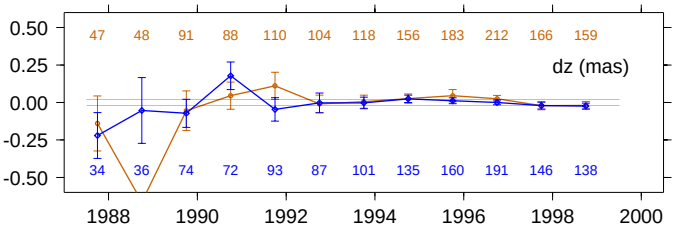

Fig. 11. Relative equatorial bias of yearly CRFs, before (yellow/light) and after (blue/heavy) the implementation of the stabilizing algorithm. The double horizontal line corresponds to the stated uncertainty of the ICRF axes directions (± 20 μas).

4. Comparison of source quality criteria

The stabilization process described in Sect. 3 is one possible way to select the sources that would form the core of a high stability celestial reference frame based on a least square analysis of VLBI source coordinates. We also presented in Sect. 2 a set of quality estimators based on various statistics. These criteria and the current ICRF ones are summarized and compared in Table 4. Seven quality criteria are considered. The set of sources is partitioned according to each qualifier. The classifications retained to discriminate between the "good" and "bad" sources according to qualifiers 4, 5, and 6 are based on their distributions (see respective Figs. 6, 8 and 5). Those for qualifiers 1, 2, 3 and 7 are self explanatory. For each qualifier, the table gives the number of sources of Table 2 for which the statistics could be performed, and the percentage of those kept by the stabilizing algorithm. The percentages of sources kept is printed in bold for the "good" sources according to the qualifier. The following comments can be made.

1. ICRF categories. The first pair of columns corresponds to the sources belonging to the selection of sources used in this study (Table 2). The numbers in brackets correspond to the complete set of these sources in ICRF-Ext.1. The stability test retains practically all definition and candidate sources, and most of the others. When considering numbers of sources and the percentages relative to the complete ICRF-Ext.1, one can note first that only 1/3 of the "candidate" sources were selected on the basis on long and dense observational history. In fact we know that a number of candidate sources are considered so because their time span of observation is still too short. We also know that a number of sources qualified as "other" had a rich observational history, explaining the selection of 3/4 of them. The selection rate of the "definition" sources is between the other two (1/2). Already at this first level, the first part of our selection scheme provides a pre-qualification of sources which is quite different from the current ICRF one. Once this first selection is performed, the second one, based on the internal consistency of the time series of coordinates in the direction of the maximum variability, retains nearly

Table 4. Match of the stability selection (based on the goodness of fit of yearly coordinates) with other source qualifiers.

Criteria		No of sour.	Kept	No of sour.	Kept
1. ICRF categories:					
	Definition	108	**95%**	(212)	(**49%**)
	Candidates	98	88%	(294)	(29%)
	Other	73	67%	(102)	(48%)
2. Declination zone:					
	$+20°/+90°$	122	**85%**		
	$0°/+20°$	75	85%		
	$-20°/0°$	41	83%		
	$-90°/-20°$	45	89%		
3. ICRF structure index (X):					
	1	49	**86%**		
	2	87	80%		
	3	63	87%		
	4	26	85%		
4. χ^2		$\alpha\cos\delta$		δ	
< 2.5 ($\alpha\cos\delta$)	< 3.0 (δ)	69	**71%**	75	**64%**
> 2.5 ($\alpha\cos\delta$)	> 3.0 (δ)	22	45%	16	69%
5. One-year Allan standard error: (limits are given in mas)		$\alpha\cos\delta$		δ	
< 0.25 ($\alpha\cos\delta$)	< 0.20 (δ)	96	**80%**	92	**77%**
> 0.25 ($\alpha\cos\delta$)	> 0.20 (δ)	48	77%	52	83%
		x-axis		y-axis	
< 0.20 (x-axis)	< 0.10 (y-axis)	78	**82%**	102	**85%**
> 0.20 (x-axis)	> 0.10 (y-axis)	66	76%	42	62%
6. Rates along the local axis of maximum variability (x-axis):					
	< 0.04 mas/a	79	**72%**		
	> 0.04 mas/a	65	88%		
7. Noise spectrum:		x-axis		y-axis	
	White	25	**68%**	33	**61%**
	Flicker	20	40%	12	42%

all "definition" and "candidate" sources, thus confirming their current ICRF status. Meanwhile, 7/10 of the "other" sources are still kept. This seems to indicate that using time series information might bring in more sources that would contribute to stabilize the celestial reference frame.

2. The four declination zones considered have similar performances in the selection, suggesting that a weighting of sources derived from the goodness of fit might adequately temper the residual declination errors.
3. The structure index for each source is computed by Fey & Charlot (2000) on the basis of one map obtained during the time span covered by this study. It qualifies the level of position disturbance expected at the date of the map (1 for the less disturbed, 4 for the most disturbed). The lack of correlation between this index and our stability criterion might indicate that, in the data set used for this study, the observational and analysis errors due to other factors in general dominate the source structure effect.
4. χ^2 test. Only the 108 sources observed in more than 100 sessions could be submitted to this test. These most observed sources have an overall selection rate ($91/108 = 84\%$) smaller than that of the global set of sources (86%). This may be associated with sources observed from the early years and kept in the program in spite of a poor stability.
5. The Allan standard error at the one year interval does not particularly correlate with the stability characterized by the goodness of fit, except for the direction of the local y-axis.
6. Rates. The criterion of high versus low rates along the local x-axis does not correlate with our stability goodness of fit criterion.

7. Noise spectrum. The sources for which the Allan variance stability test could be performed are those with a long and dense observational history. As in the case of the χ^2 test, their selection rate is low (75%), probably for the same reason. However, for this limited sample, the white noise diagnosis correlates better with the stability test than does the flicker noise.

5. Summary and conclusions

This study aimed to describe in some detail the time behaviour of extragalactic radio source coordinates measured by VLBI. It is based on the 283 best observed sources over 1987.25–1999.25, extracted from 645 time series of equatorial coordinates computed for over 2000 sessions starting in 1979.

The non circular character of the measurement noise, attributable to troposphere mismodelling and/or to source structure perturbations, was highlighted. Time series of coordinates of sources south of 20° of declination are dominated by noise in declination.

To study the effective stability of the sources, we defined a local reference frame with x-axis in the direction of the maximum variability with time. We then performed a series of statistical tests whose results are compared in Table 4.

Using an original algorithm, we selected a set of 242 sources that define a time series of yearly reference frames over 1987–1998 achieving a global stability of the axes of 14 μas over the 12 years, a number comparable to the stated 20 μas axis stability of the ICRF. The last six years, however, show a large improvement in stability, with a global axes stability of 4 μas over six years.

The algorithm presented first selects sources with a long and dense history over 1987–1999 and then keeps the 86% of those with the best stability in time (or repeatability) in the direction of maximum local variability. The convergence criterion is applied on the rotation angles of yearly reference frames estimated on one hand by weighted least squares (the method used in the compilation of ICRF), and on the other hand by minimizing the L1 norm (a more robust method). The splitting of data in time-like batches also includes variations between the yearly sets of sources (see the numbers of sources in Fig. 10), so that the convergence reached has also a meaning with respect to the internal composition of the frame.

The source selection based on the stability criterion derived in this paper matches only partially the current ICRF qualification, while it has the advantage of being based on a statistical approach. It allows the safe introduction of previously dubious sources while providing a similar accuracy in the definition of axes.

The present study also highlights the usefulness of considering the time evolution of radiosource directions, not only for internal purposes such as the ICRF quality control or applications like differential VLBI, but also to enhance the support of VLBI for scientific research, for example, in the understanding of the physical properties of the non-rigid Earth through analysis of precession and nutation observations (Dehant et al. 2000), or for realistic studies of source structure or microlensing effects. Future astrometry space missions are expected to provide directions of extragalactic objects in optical wavelengths with an accuracy that competes with that of VLBI. When these results become available, the high accuracy unification of Earth- and space-based celestial reference frames will require that the VLBI results reach their maximum precision and accuracy.

References

Allan, D. W. 1966, Proc. IEEE, 54, 221

Bevington, P. R. 1969, Data reduction and Error analysis for the physical sciences (McGraw-Hill, New York)

Charlot, P., & Sovers, O. J. 1997, The New International Celestial Reference Frame, 23rd IAU GA, JD 7, August 1997, Kyoto, Japan

Dehant, V., Feissel, M., de Viron, O., et al. 2000, 24th IAU GA, JD 2, August 2000, Manchester, UK

Feissel, M., Gontier, A.-M., & Eubanks, T. M. 2000, A&A, 359, RN1201

Feissel, M., & Mignard, F. 1998, A&A, 331, L33

Fey, A. L., & Charlot, P. 1997, ApJS, 111, 95

Fey, A. L., & Charlot, P. 2000, ApJS, 128, 17
`http://www.observ.u-bordeaux.fr/public/radio/PCharlot/structure.html`
`http://maia.usno.navy.mil/RRFID/`

International VLBI Service (IVS), 1999, 1999 IVS Annual Report, NASA/TP-1999-209243, 227

International Earth Rotation Service (IERS), 1999, 1998 Annual Report, Observatoire de Paris, 83
`ftp://hpiers.obspm.fr/iers/icrf/iau/icrf-Ext.1/README.ICRF-EXT1`

Ma, C. 2000, IVS General Meeting proceeding, NASA/CP-2000-209893, 52

Ma, C., Arias, E. F., Eubanks, et al. 1998, AJ, 116, 516

Ma, C., & Feissel, M., (ed.) 1997, IERS TN 23, Observatoire de Paris

McMillan, D. S., & Ma, C. 1997, GRL, 24, 453

Rutman, J. 1978, Proc. IEEE, 66, 1048